Received: 14 March 2019 | Revised: 11 May 2019 | Accepted: 13 May 2019

DOI: 10.1002/psc.3194

RESEARCH ARTICLE

WILEY Journal of PeptideScience

The 1,3-diyne linker as a rigid "*i*,*i*+7" staple for α-helix stabilization: Stereochemistry at work

Steven Verlinden[1] | Niels Geudens[2] | Kevin Van holsbeeck[1,2] | Morgane Mannes[1] | José C. Martins[2] | Guido Verniest[1,3] | Steven Ballet[1]

[1] Research Group of Organic Chemistry, Department of Chemistry and Department of Bioengineering Sciences, Faculty of Sciences and Bioengineering Sciences, Vrije Universiteit Brussel, Brussels, Belgium

[2] NMR and Structure Analysis Unit, Department of Organic and Macromolecular Chemistry, Ghent University, Ghent, Belgium

[3] Predictive Analytics and Stability Sciences, Center of Excellence, CRS, Analytical Development, PDMS, DPDS, Janssen Research and Development, Janssen Pharmaceutical Companies of Johnson & Johnson, Beerse, Belgium

Correspondence
Guido Verniest and Steven Ballet, Research Group of Organic Chemistry, Department of Chemistry and Department of Bioengineering Sciences, Faculty of Sciences and Bioengineering Sciences, Vrije Universiteit Brussel, Pleinlaan 2, B-1050 Brussels, Belgium.
Email: guido.verniest@vub.be; steven.ballet@vub.be

José C. Martins, NMR and Structure Analysis Unit, Department of Organic and Macromolecular Chemistry, Ghent University, Krijgslaan 281-S4, 9000 Ghent, Belgium.
Email: jose.martins@ugent.be

Funding information
Fonds Wetenschappelijk Onderzoek; Research Council of the Vrije Universiteit Brussel; Research Foundation Flanders

Short alphahelical peptide sequences were stabilized through Glaser-Hay couplings of propargylated L- and/or D-serine residues at positions *i* and *i*+7. NMR analysis confirmed a full stabilization of the helical structure when a D-Ser (i), L-Ser (*i*+7) combination was applied. In case two L-Ser residues were involved in the cyclization, the helical conformation is disrupted outside the peptide's macrocycle.

KEYWORDS

constrained peptides, Glaser-Hay coupling, helix stabilization, peptide stapling

1 | INTRODUCTION

Protein-protein interactions (PPIs) control essential cellular processes and influence several biological functions.[1] However, despite their fundamental roles, PPIs are considered to be rather cumbersome targets for drug design because the large and often flat contact surfaces involved are not easily hijacked by small molecules. Nonetheless, the modulation of PPIs is important for the elucidation of biological processes, and it represents a promising strategy towards next-generation therapeutics.[2] One approach for the rational design of PPI inhibitors consists of a structure-based approach, wherein the topology of protein epitopes can serve as a starting point.[3] Whereas a PPI takes place over a large interaction surface area—typically 750 to 1500 $Å^2$—[4] only a few key residues usually contribute to the majority of the binding affinity.[5] These epitopes are often defined by the secondary structure of the underlying amino acid chain.[1] More specifically, α-helices are key recognition domains in many naturally occurring PPIs, and hence, their mimicry has received great attention during the past decade.[1,3,6] When helical peptide segments are extracted from their protein context, a significant loss in

conformational homogeneity is standardly observed, and hence, there is a need for secondary structure stabilization. Among the different successful strategies described to date, the stabilization of α-helical peptide conformations can be accomplished by introducing covalent links between amino acid side chains at selected positions.[6] As a result, these "stapled" peptides are often characterized by an improved binding affinity, metabolic stability, and enhanced cell penetration, as compared with their linear peptide counterparts.[7,8] When aiming at α-helix mimetics, a macrocyclization involving the amino acids side chains at the *i*,*i*+4 or *i*,*i*+7 positions is commonly employed to bridge one or two helical turns, respectively.[1,5,9] Whereas a vast amount of work has been done on *i*,*i*+4 cyclizations,[10] the current report focusses on the tethers bridging two turns via an *i*,*i*+7 cyclization. The *i*,*i*+4 and *i*,*i*+7 tethers complement each other, as distinct properties in structuration can be observed. Schafmeister et al reported, for example, on a ring-closing olefin metathesis (RCM) crosslinked peptide, where stapling at position *i*,*i*+4 neither stabilized nor destabilized the helix, hydrocarbon stapling at positions *i*,*i*+7 resulted in significant stabilization of the α-helical structure.[11] Fujimoto et al showed that the α-helical predisposition of short peptides can be stabilized with acetylenic crosslinkers reacted with Lys residues at positions *i*,*i*+4 and *i*,*i*+7. The peptides stapled at positions *i*,*i*+4 showed an α-helical content up to only 35%, whereas in *i*,*i*+7-tethered analogues, the α-helical content increased to 65%, as monitored by circular dichroism (CD).[12]

One of the first *i*,*i*+7 conformationally constrained helical peptides was obtained by disulfide formation between 2-amino-6-mercaptohexanoic acid residues with mixed D- and L-configurations at the associated positions (Figure 1A). The obtained cyclic peptide, with a flexible 10 atom long linker, displayed an increased helicity, as compared with the acyclic counterpart.[13] Similarly, bisarylmethylene bromides were used to introduce rigid tethers connecting two cysteine residue side chains at position *i*,*i*+7, which resulted in cyclic analogues with increased helicity and bioactivity.[20,21] The photoswitchable azobenzene moiety has also been used as a thiol-based crosslink overarching two helix turns (Figure 1B). Upon stapling at positions *i* and *i*+7, the α-helical conformation was clearly more pronounced when the azobenzene moiety is in the *cis* configuration.[14,15] Additionally, Fujimoto et al successfully investigated nine different rigid *i*,*i*+7 stapling moieties, encompassing short alkylene-, benzene-, and biphenylene-based bridges (not shown), and demonstrated that insertion of such elements could indeed provide enhanced helicity for some of the analogues.[22] Improved helicity could also be obtained by installing a bisamide crosslink through the reaction of two glutamic acid residues at positions *i* and *i*+7 with a diamino building block (Figure 1C).[16,17] Different copper-catalyzed azide-alkyne cycloaddition (CuAAC) was successfully applied to stabilize α-helices. Two triazoles could, for example, be introduced by reacting azidolysines at positions *i* and *i*+7 with aromatic dialkynes resulting in the "double-click" stapling of a peptide (Figure 1D).[18,19] By introducing all-hydrocarbon stapling, Verdine and coworkers exploited a powerful tool for the stabilization of α-helices: incorporation of α-methyl-α-alkenylamino acids followed by RCM results in the formation of stapled peptides.[23,24] The C11 linker afforded by combination of an R- and S-configured α-methyl-α-alkenylamino acid at position *i* respectively *i*+7 appeared optimal for bridging two turns in a helix (Figure 1E).[11]

In recent years, several studies report the use of 1,3-diynes, obtained through Glaser-Hay alkyne-alkyne coupling, for both peptide secondary structure stabilization and biorthogonal labeling.[25-30]

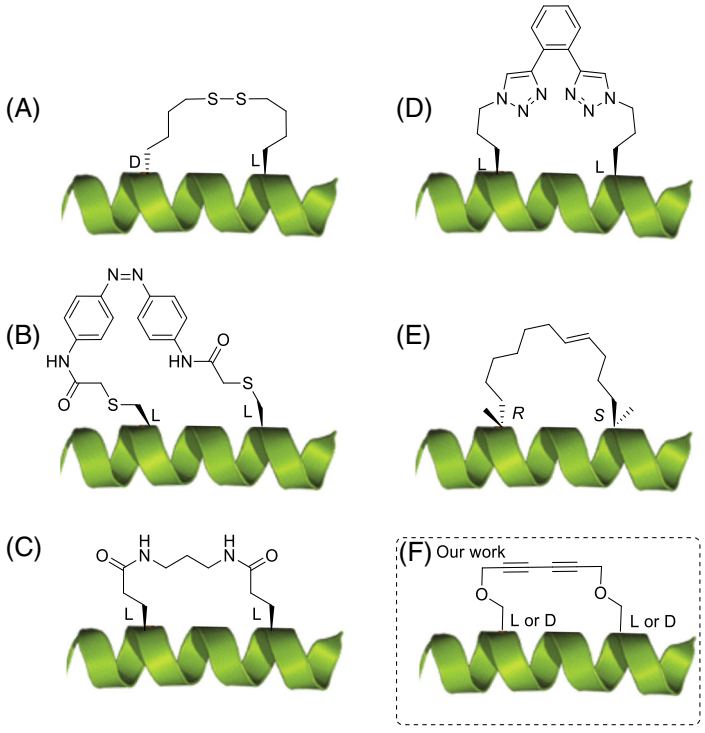

FIGURE 1 Selected examples of *i*,*i*+7 staples involving A, the disulfide linkage of D- and L-2-amino-6-mercaptohexanoic acid[13]; B, an azobenzene linkage between two cysteine residues[14,15]; C, a double lactam bridge between two glutamic acid residues[16,17]; D, a double-click stapling between two 5-azido-2-aminopentanoic acid and an aromatic dialkyne[18,19]; E, ring-closing olefin metathesis (RCM) stapling between two α-methyl olefin amino acids[11]; and F, the 1,3-diyne linker between two *O*-propargylated serine residues with D- or L-configuration

In light of this increasing interest of alkyne-alkyne couplings in peptide chemistry, our group examined the use of *O*-propargylated serine residues towards the *i*,*i*+7 stabilization over two helical turns (see Scheme 1F). In parallel to this work, Cistrone et al showed an intramolecular coupling of L-*O*-propargylated serines for the stapling of BCL-9 α-helical peptides.[29] Several 1,3-diyne tether lengths were evaluated (*i*,*i*+4, *i*,*i*+5, *i*,*i*+6, and *i*,*i*+7), and it was concluded that the Glaser coupling using copper chloride, the 4,4′-bis (hydroxymethyl)-2,2′-bipyridine ligand, and diisopropylethylamine was most efficient for *i*,*i*+4 stapling (>95% conversion), whereas the degree of macrocyclization conversion significantly decreased when longer tethers were introduced. With regard to helical content, the *i*,*i*+4 and *i*,*i*+7 constraints led to improved helicities of 56% and 40%, respectively, for the studied 23-mer.[29]

To complement the latter study, in this work, α-helices were efficiently stabilized with a 1,3-diyne staple, resulting from *O*-propargylated serine residues at the *i*,*i*+7 positions, but importantly, the influence of the *O*-propargylated serines' configuration on the α-helical propensity and structure was evaluated by means of CD, nuclear magnetic resonance (NMR), and molecular modeling.

In search for a suitable model system, stapled peptide analogues able to inhibit MDM2 and MDMX proteins, important regulators of the transcriptional activity and stability of p53, were selected.[31] Within this context, Chang et al designed an α-helical peptide (ATSP-7041) encompassing an all-hydrocarbon staple, which proved to be a highly potent dual inhibitor of both MDM2 and MDMX.[32] We employed the same 12-mer peptide as a model system and replaced the α-methyl-α-alkenyl amino acids in ATSP-7041 with *O*-propargylated serines for the evaluation of the 1,3-diyne linker as a rigid staple for *i*,*i*+7 α-helix stabilization.

2 | MATERIALS AND METHODS

2.1 | General

Column chromatography purifications were conducted on silica gel 60 (40-63 μm; Grace Davisil). Thin-layer chromatography (TLC) was carried out on glass plates precoated with silica gel 60F254 (Merck); the spots were visualized under UV light (λ = 254 nm), and/or $KMnO_4$ (aq) was used as the revealing system. Preparative high-performance liquid chromatography (HPLC) was conducted using a Gilson semipreparative HPLC equipped with a Supelco Discovery Bio Wide Pore C18 column or on a Knauer system equipped with a ReproSil-Pur ODS-3 column (150 mm × 16 mm, 5 μm). Samples were analyzed on a VWR-Hitachi Chromaster HPLC, equipped with a Chromolith HighResolution RP-18 endcapped column (50 mm × 4.6 mm, 1.1 μm, 150 Å; or 150 mm × 4.6 mm, 1.1 μm, 150 Å). Eluting products were detected by a Chromaster HPLC 5430 diode array detector at a wavelength of 214 nm. The solvent system consists of 0.1% trifluoroacetic acid (TFA) in ultrapure water and 0.1% TFA in acetonitrile. The samples were then eluted through the column using a gradient ranging from 1% acetonitrile to 100% acetonitrile more than 6 minutes runtime at a flow rate of 3.0 or 2.8 mL min^{-1}. Melting points were acquired on a Buchi Melting Point B-540 and are uncorrected. IR absorption spectra were recorded on a Thermo Nicolet 700 FT-IR spectrophotometer. $[\alpha]_D^{20}$ values were obtained on a Polartronic M Schmidt-Haensch polarimeter calibrated at 20°C. NMR measurements were performed on a Bruker Avance II spectrometer either operating at ^1H and ^{13}C frequencies of 500.13 and 125.76 MHz or 700.13 and 176.04 MHz and respectively equipped with a 5-mm BBI-Z probe and a 5-mm Prodigy TCI probe. When using MeOH-*d*3, the OH-signal was suppressed using excitation sculpting.[33] The sample temperature was set to 298.2 K. Standard pulse sequences as present in the Bruker library were used throughout, unless stated otherwise. High precision 5-mm NMR tubes (Norell, Landisville, NJ) were used. ^1H and ^{13}C chemical shift scales were calibrated by using the residual solvent signal using trimethylsilyl (TMS) as secondary reference. Two-dimensional spectra measured for structure elucidation include a 2D ^1H-^1H DQF-COSY, 2D ^1H-^1H TOCSY with a 90-millisecond MLEV-17 spinlock, 2D ^1H-^1H off-resonance ROESYs with 200-millisecond mixing time, and gradient-selected ^1H-^{13}C gHSQC and gHMBC. Typically, 2048 data points were sampled in the direct dimension for 512 data points in the indirect dimension, with the spectral width set to 11 and 110 ppm along respectively the ^1H and ^{13}C dimension. The ^1H-^{13}C HMBC was measured with a 210-ppm ^{13}C spectral width. For 2D processing, the spectra were zero filled to a 2048 × 2048 real data matrix. Before Fourier transformation, all spectra were multiplied with a squared cosine bell function in both dimensions or sine bell in the direct dimension for the gHMBC.

High-resolution mass spectrometry was conducted on a Waters Micromass QTof in ES+ mode, using reserpine as the reference. CD spectra were measured using a quartz cuvette of 1-mm path length at 20°C on a Jasco J-715 spectropolarimeter with a scan rate of 50 nm min^{-1}, a bandwidth of 1.0 nm for a resolution of 0.5 nm. All peptides were dissolved in methanol at a concentration of 100μM. Five baseline scans of buffer were taken and averaged at T = 20°C, followed by five scans of each peptide. These spectra were averaged, baseline-subtracted from the average blank scans, and converted to the mean residue ellipticity. Commercial amino acids and coupling reagents were purchased from Novabiochem and Chem-Impex. 4,4′-bis (hydroxymethyl)-2,2′-bipyridine was purchased from TCI and dimethylsulfoxide (DMSO) from ABCR. All other used reagents and chemicals were purchased from Sigma Aldrich and used without further purification unless otherwise specified.

2.2 | Peptide synthesis

A representative synthesis is given for the preparation of cyclic peptide **7** through (a) macrolactamization and (b) Glaser-Hay alkyne-alkyne coupling.

a. Cyclic analogues through macrolactamization

Linear fragment **5** was synthesized manually by the N_α-Fmoc methodology on Rink amide resin (0.11 mmol, loading 0.47 mmol/g)

using (2-(6-chloro-1*H*-benzotriazole-1-yl)-1,1,3,3-tetramethylaminium hexafluorophosphate) (HCTU)/DIPEA as a coupling reagent. Fmoc-AA-OH (4 equiv), HCTU (4 equiv), and DIPEA (5 equiv) in dimethylformamide (DMF) were added to the swollen solid support, and the reaction mixture was shaken for 1 to 2 hours. For diyne dipeptide **4**, 1.5 equiv of the Fmoc-AA-OH was dissolved in DMF with HCTU (1.5 equiv) and DIPEA (1.5 equiv), and the reaction mixture was shaken for 15 hours. Trityl was used as a side chain protecting group for Fmoc-Gln-OH, tert-butyloxycarbonyl was used as a side chain protecting group for Fmoc-Trp-OH, and tert-butyl was used as the Fmoc-amino side chain protecting group for Fmoc-Ser-OH, Fmoc-Tyr-OH, and Fmoc-Thr-OH. The resin was washed three times with DMF and three times with CH_2Cl_2. Completion of the reaction was tested by the Kaiser test. In the case of a positive color test, the coupling was repeated until a negative color test was obtained. Fmoc deprotection was carried out using 20% 4-methylpiperidine in DMF. After Fmoc deprotection of the final coupled Fmoc-AA-OH, saponification of the methyl ester was achieved by adding a 2M $LiOH.H_2O$ solution (10 equiv) in H_2O/DMF 3:7 to the resin, and the reaction mixture was shaken for 3 hours. Completion of the reaction was determined through liquid chromatography–mass spectrometry (LC-MS) analysis. Subsequently, lactamization was achieved by adding a mixture of PyBOP (3 equiv) and DIPEA (6 equiv) in DMF to the resin, and the reaction mixture was shaken for 15 hours. The resin was washed three times with DMF and three times with CH_2Cl_2. Completion of the reaction was determined through LC-MS analysis. The Alloc protecting group was removed by adding a mixture of Pd $(PPh_3)_4$ (0.2 equiv) and morpholine (10 equiv) in CH_2Cl_2, and the reaction mixture was shaken for 2 × 10 minutes to afford **6**. The resin was washed three times with DMF, three times with CH_2Cl_2, three times with sodium diethyldithiocarbamate, and two times with pyridine hydrochloride. Completion of the reaction was determined through LC-MS analysis. The final three amino acids were added through regular Fmoc-SPPS as explained above. After Fmoc deprotection of the final coupled Fmoc-AA-OH, the free amine was acetylated by adding Ac_2O/CH_2Cl_2/DIPEA (0.5:8:1) to the resin, and the resin was shaken for 1 hour. The final cleavage of the peptide from the resin was accomplished by treatment with TFA/triethylsilane (TES)/H_2O 95:2.5:2.5 for 2 hours. The crude peptides were obtained by filtration, lyophilized, and purified via preparative RP-HPLC to obtain **7** as a white powder.

b. Cyclic analogues via Glaser-Hay macrocyclization

Linear protected peptides were synthesized with the automated *N*-Fmoc methodology on a Sieber amide resin (0.10 mmol, loading 0.7 meq/g) with a Liberty Blue Automated Microwave Peptide Synthesizer. Fmoc deprotections were performed by treatment with 20% 4-methylpiperidine in DMF for 1.05 minutes at 90°C under microwave conditions. Couplings were carried out with 4 equiv of Fmoc-protected amino acids, 4 equiv of DIC (0.5M in DMF), and 4 equiv of Oxyma (1M in DMF) for 2.1 minutes at 90°C under microwave conditions. The resin-bound peptides were subsequently acetylated manually using acetic anhydride (50 equiv) and DIPEA (50 equiv) in DMF (5 mL) for 30 minutes. The fully protected peptides were eventually cleaved using 1% TFA in dichloromethane (DCM) for 50 minutes. The filtrates were concentrated in vacuo, lyophilized, and directly used without intermediate purification. For the subsequent Glaser-Hay cyclization, 4,4′-bis (hydroxymethyl)-2,2′-bipyridine (bpy-diol) (16 equiv) and CuCl (12 equiv) were dissolved in DMSO (15 mL), followed by the addition of 40.0 mg of the crude linear fully protected peptide (0.02 mmol) in DMSO (5 mL). After the addition of DIPEA (20 equiv), the mixture was heated to 40°C and stirred for 24 hours. The reaction mixture was diluted with 40 mL water to precipitate the cyclized peptides. The precipitate was collected via centrifugation and decantation and subsequently washed a few times with water. To the obtained precipitates, 10 mL of the cleavage cocktail TFA/TIS/water 95/2.5/2.5 was added. After stirring the solution for 1.5 hours at room temperature, it was concentrated in vacuo and lyophilized. Subsequent purification with preparative RP-HPLC yielded respectively 2.5 and 1.8 mg of **7** and **8**.

2.3 | Structure determination

Following complete ^1H and ^{13}C assignment of **7** and **8** at 700 MHz (see the Supporting Information), off-resonance 2D ^1H-^1H ROESY spectra were recorded in MeOH-*d*3 for structure calculation. The optimal mixing time to develop rOe's during the spinlock was determined by measuring the buildup of the intensity of a handful of rOe's as a function of the spinlock mixing time in a series of short duration off-resonance 2D ^1H-^1H ROESY spectra (Figures S5 and S6). All relevant cross-peaks were manually assigned and integrated using the CCPN software v2.0.5.[33] For the conversion of rOe intensities into distances, a calibration against the average of the integrals of all rOe intensities was used within CCPN, with the usual reference average distance of 3.2 Å.

To generate an initial set of conformations, a standard simulated annealing protocol in AMBER was performed using the ff14SB force field, whereby rOe distance information was included as restraints. Subsequently, a 100-nanosecond nonrestrained molecular dynamics (MD) simulation was performed in explicit methanol using periodic boundary conditions, by way of refinement step. Bond lengths involving hydrogen were held fixed with the SHAKE algorithm. Temperature scaling was performed using Langevin dynamics with a collision frequency of 1.0 ps^{-1} while electrostatic interactions were computed using the particle mesh Ewald summation. A cutoff for nonbonded interactions of 12 Å was used. Prior to unrestrained MD, a short standard equilibration protocol was applied consisting of a two-step energy minimization. In the first stage, the solute molecules are fixed with a strong positional restraint (500 kJ mol^{-1}), and only the positions of the solvent are minimized. Subsequently, in the second stage, the entire system is minimized without the application of restraints. After these minimizations, the systems are allowed to heat up from 0 to 300 K. In order to ensure this occurs without any wild fluctuations in the solute, a weak potential energy restraint (10 kJ mol^{-1}) is

applied on the solute molecules. This step is performed at constant volume to minimize inaccuracies in the beginning of the simulation, where the temperature is very low. Finally, production runs were performed using constant pressure dynamics with isotropic position scaling. All MD simulations were run on a single GTX780 GPU using the GPU implementation of pmemd provided in the AMBER14 simulation package. The calculated trajectories were visualized using VMD 1.9.1[34] while in-depth analysis was performed using cpptraj[35] provided with the AMBER software.

A cluster analysis protocol was used to select the 3D conformation that ideally reflects the time-averaged position of the atomic coordinates. More specifically, following the calculation of the pairwise atomic coordinate rootmean square deviations (RMSDs) between the conformations manifesting throughout the trajectory, the built-in DBSCAN [*x*+1] algorithm of cpptraj assembles a cluster of the trajectory's converged conformations, while the "nonrelaxed" structures in terms of molecular geometry are perceived as noise in the simulation and become omitted. In parallel, the algorithm allows determining the conformation for which the atomic coordinate RMSD (using all the atoms in the molecule) is minimal in comparison with those averaged over the whole cluster of converged conformations. This conformation is then used as a representative of the dominant cluster present in MD trajectory.

3 | RESULTS AND DISCUSSION

Prior to this work, we reported β-turn stabilizing macrocycles, obtained via Glaser-Hay couplings involving Ser side chains equipped with terminal alkynes.[24,25] By application of the optimal reaction conditions reported in this previous work (ie, Cu $(OAc)_2.H_2O$, $NiCl_2$, Et_3N, Py, O_2, 60°C, EtOH or DMF), cyclization of the linear model peptide Ac-Leu-Thr-Phe-Ser(*O*-propargyl)-Ala-Tyr-Trp-Ala-Gln-Leu-Ser(*O*-propargyl)-Ser-NH_2 in solution as well as on solid support was attempted. However, in both cases, the alkyne-alkyne coupling failed to generate the cyclized peptide sequence to any significant extent. Therefore, two cyclization strategies were considered and optimized in parallel. Next to the Glaser-Hay macrocyclization, a macrolactamization approach was considered, wherein the 1,3-diyne staple would be introduced prior to cyclization through the introduction of a diyne-bearing dipeptide, to be used in regular SPPS.

3.1 | Synthesis and structure analysis of stapled peptides by macrolactamization

To access the required dipeptide building block (Scheme 1), Cadiot-Chodkiewicz reaction conditions were first evaluated (see the Supporting Information for more detail) to couple bromoalkyne **1a** and terminal alkyne **2** towards the formation of unsymmetrical diyne **3**, but the desired compound could only be isolated in less than 5% yield under the applied conditions. Hence, Glaser-Hay conditions were used to couple terminal alkynes **1b** and **2**. Using 3 equiv of **2** and 1 equiv of **1b** in the presence of Cu $(OAc)_2.H_2O$, $NiCl_2$, Et_3N, and pyridine in EtOH under an oxygen atmosphere, compound **3** was formed in 55% isolated yield after 4 hours of reaction time at room temperature. Under these reaction conditions, homodimerization of terminal alkynes **1b** and **2** was also observed, but both types of homodiynes were easily separated in 6% and 17% yield from heterodiyne **3** via silica gel chromatography. Concomitant Boc- and *tert*-butyl deprotection after TFA treatment and subsequent Fmoc-protection led to the formation of the SPPS-compatible dipeptide **4**.

Dipeptide **4** was then used as a building block in regular Fmoc-SPPS on Rink amide resin (Scheme 2). After assembly of the first subsequence **5**, saponification of the methyl ester on resin was performed using the conditions developed by Cantel et al (10 equiv of LiOH in tetrahydrofuran [THF]/H_2O).[36] However, in our hands, a solvent system switch to H_2O/DMF 1:1 improved the conversion to the desired carboxylic acid. In a next step, lactamization was achieved after 15 hours by adding 3 equiv of PyBOP and 6 equiv of DIPEA in DMF as a coupling mixture and followed by Alloc-deprotection with Pd $(PPh_3)_4$ and morpholine as nucleophilic scavenger. Noteworthy, when using phenylsilane as a scavenger, partial reduction of the 1,3-diyne was observed. Finally, the final three amino acid residues were added, followed by acetylation of the terminal amine, cleavage from the resin, and purification via preparative RP-HPLC, yielding cyclic peptide **7**.

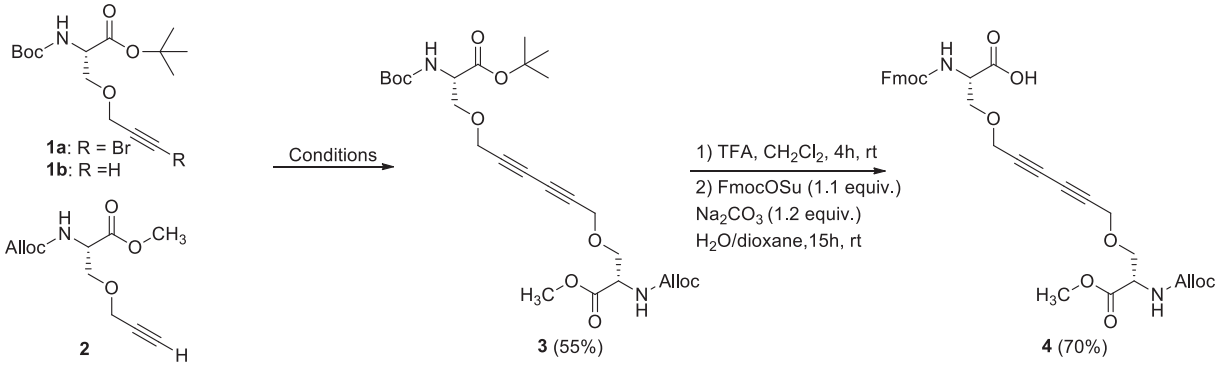

SCHEME 1 Synthesis of the dipeptide diyne building block **4**. Conditions: R = Br (Cadiot-Chodkiewicz reaction): see all attempted conditions in the electronic supporting information. Diyne **3** isolated in <5% yield; R = H (Glaser-Hay reaction): **1b** (1 equiv), **2** (3 equiv) Cu $(OAc)_2.H_2O$ (0.5 equiv), $NiCl_2$ (0.5 equiv), Et_3N (3 equiv), pyridine (5 equiv), O_2, EtOH, 4 h, rt

Colour online, B&W in print

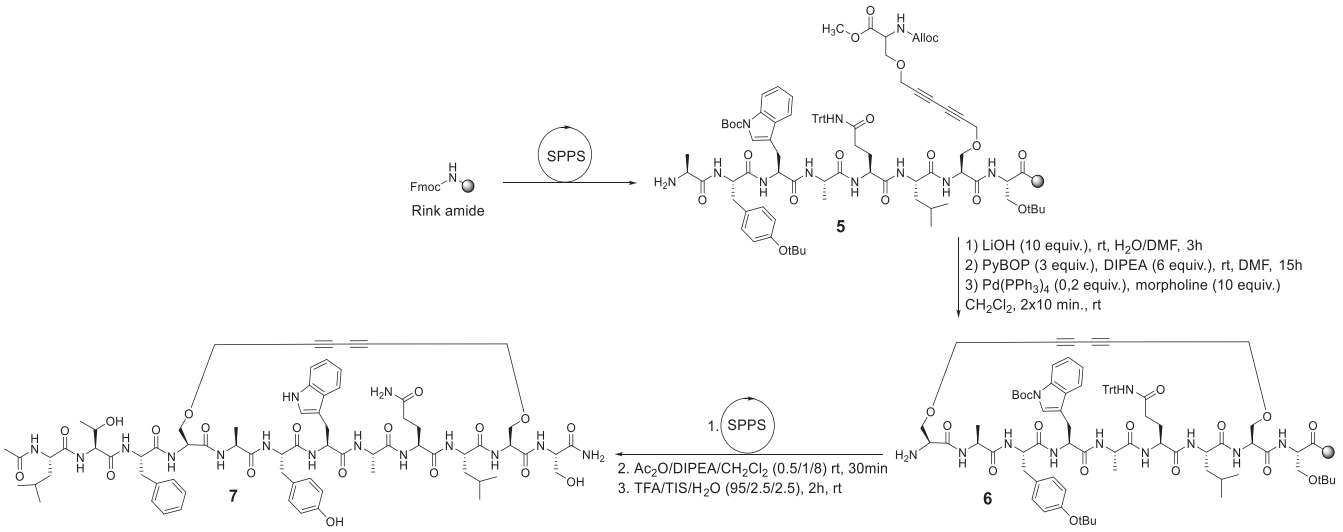

SCHEME 2 Synthesis of cyclic peptide **7** through macrolactamization

To evaluate the importance of the *O*-propargylated serine residues' configuration on the stabilization of helicity, a synthesis of the three other diyne-bearing dipeptides with altered configurations (ie, [D-Ser^4,L-Ser^{11}] **8**, [L-Ser^4,D-Ser^{11}] **9**, and [D-Ser^4,D-Ser^{11}] **10**) was attempted (Figure 2). Although all desired analogues were seemingly obtained as determined by HPLC-MS analysis, NMR would eventually demonstrate that the chiral center at position 4 was subject to epimerization (see discussion below) and hence quasi fully epimerized compound **8**, providing mostly compound **7**, was accessed through this synthetic approach.

Nonetheless, the helical character of the obtained products was first screened by CD spectroscopy (see the Supporting Information). Because the peptide analogues bearing a L-Ser^{11} residue showed a more pronounced helical character, represented by two fingerprint minima around 208 and 220 nm for α-helical peptides (Figure S11), the D-Ser^{11} compounds (**9** and **10**) were not considered any further during the subsequent NMR analyses.

The above-mentioned epimerization of the Ser^4 residue was noted via an in-depth NMR analysis performed for cyclic peptides with a L-Ser^{11} residue. A characteristic TOCSY pattern could be identified, starting from the amide resonance, for each of the 12 amino acids in both peptides. Moreover, the sequence of the individual amino acids could be confirmed through identification of the $H^N(i)$–$H^N(i\pm1)$ and $H^\alpha(i)$–$H^N(i+1)$ correlations in the ROESY spectrum and independently using the $H^N(i)$–$C'(i-1)$ correlations in the ^{1}H-{^{13}C} gHMBC spectrum. The diyne linkage between Ser^4 and Ser^{11} could be established using the $^nJ_{CH}$ cross-peaks connecting Ser^4 H^β and Ser^{11} H^β with the respective adjacent methylene carbons of the diyne linker. Consequently, a full NMR assignment could be achieved (Tables S3 and S4). Surprisingly, the ^{1}H and ^{13}C chemical shift values of both peptides were found to be quasi identical, with identical backbone H^N and $H^\alpha C^\alpha$ fingerprints in the 1D ^{1}H and 2D ^{1}H-{^{13}C} gHSQC, respectively. However, the L/D switch in configuration expected for the targeted analogues **7** vs **8** would introduce a distinct orientation of the side chain that, for a cyclic peptide, should significantly impa +ct the local chemical shifts[36-38] with differences extending throughout the entire diyne linker. We concluded that D-Ser^4 in the targeted structure **8** epimerized during chemical synthesis, yielding compound **7**. In conclusion, the lengthy strategy above suffers from many disadvantages, such as modest yields, additional synthetic steps, and most importantly, epimerization during cyclization; hence, it was abandoned.

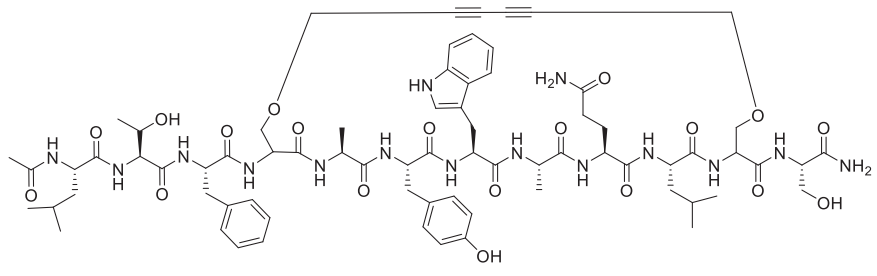

7: Ac-Leu-Thr-Phe-[L-Ser(*O*-prop.)^4-Ala-Tyr-Trp-Ala-Gln-Leu-L-Ser(*O*-prop.)^{11}]-Ser-NH_2
8: Ac-Leu-Thr-Phe-[D-Ser(*O*-prop.)^4-Ala-Tyr-Trp-Ala-Gln-Leu-L-Ser(*O*-prop.)^{11}]-Ser-NH_2
9: Ac-Leu-Thr-Phe-[L-Ser(*O*-prop.)^4-Ala-Tyr-Trp-Ala-Gln-Leu-D-Ser(*O*-prop.)^{11}]-Ser-NH_2
10: Ac-Leu-Thr-Phe-[D-Ser(*O*-prop.)^4-Ala-Tyr-Trp-Ala-Gln-Leu-D-Ser(*O*-prop.)^{11}]-Ser-NH_2

FIGURE 2 Overview of the targeted cyclic peptides **7** to **10**

3.2 | Synthesis and structure analysis of stapled peptides by Glaser-Hay coupling

Following the failed attempt with Cu $(OAc)_2.H_2O$, $NiCl_2$, Et_3N, Py, and O_2 (*vide supra*) and as a much more direct approach, the synthesis of isomers [L-Ser^4,L-Ser^{11}] **7** and [D-Ser^4,L-Ser^{11}] **8** was attempted via an on-resin *i*,*i*+7 Glaser-Hay stapling following the work of Cistrone et al, with identical reaction conditions using copper chloride, 4,4′-bis (hydroxymethyl)-2,2′-bipyridine (bpy-diol) ligand, and DIPEA in DMSO.[29] In our hands, however, both [L-Ser^4,L-Ser^{11}] **7** and [D-Ser^4,L-Ser^{11}] **8** were not obtained under these conditions; therefore, the stapling was attempted in solution. To do so, linear and fully protected peptide analogues were synthesized on a Sieber resin, followed by acetylation and cleavage from the resin (1% TFA in DCM). Eventually, the Glaser-Hay stapling was performed with modified conditions using DMSO (1mM peptide concentration), CuCl (10 equiv), bpy-diol (15 equiv), and DIPEA (20 equiv) at 40°C,[29,30] resulting in full HPLC conversion after 24 hours. Subsequent treatment with TFA/TIS/H_2O 95/2.5/2.5 and preparative RP-HPLC purification yielded the desired stapled peptides [L-Ser^4,L-Ser^{11}] **7** and [D-Ser^4,L-Ser^{11}] **8**. Under the assumption that the configuration of L-Ser^4 was not affected during the Glaser-Hay cyclization, both isomers were subjected to NMR analysis.

Full NMR characterization of **7** and **8**, obtained by Glaser-Hay cyclization, was performed in similar fashion as described above for peptide **7** (Tables S5 and S6). This time, **7** and **8** displayed clear differences in chemical shifts. Indeed, both the amide and methyl group regions of the compounds show pronounced differences, while the ^{1}H-{^{13}C} gHSQC features a clearly different H$^\alpha$C$^\alpha$ backbone fingerprint. Moreover, the ^{1}H and ^{13}C chemical shifts recorded for **7** matched with those of **7** accessed by macrolactamization, proving that all possess the same [L-Ser^4,L-Ser^{11}] configuration. Upon closer examination, the 1D ^{1}H NMR spectrum of the almost fully epimerized **8** (by macrolactamization) shows traces of the compound with the targeted [D-Ser^4,L-Ser^{11}] stereochemistry as can be seen from the match of these with **8** (by Glaser-Hay), while the main compound perfectly matches **7**. Of note, coelution of both isomers during analytical analysis and preparative HPLC purification did not allow a visualization and separation upon these analyses, respectively.

Upon assignment of all four peptides, a distance constraint–based structure calculation was performed for **7** (with [L-Ser^4,L-Ser^{11}] stereochemistry) and **8** (with [D-Ser^4,L-Ser^{11}] stereochemistry). For **7**, a total of 139 interproton distances, including 25 medium (*i* to *i*+*n* $\leq$ 4) and 19 long-range constraints (*i* to *i*+*n* > 4), were extracted from an off-resonance ROESY recorded with optimal mixing time (Table S7). All residues were involved in a sufficient number of distance restraints to engage into a structure calculation, which yielded a well-defined, converged ensemble of structures after the simulated annealing calculation. By way of unbiased refinement, a 100-nanosecond MD simulation was subsequently performed in explicit methanol solvent without imposing any restraints. Cluster analysis of the unrestrained trajectory based on **7** showed the presence of a single dominant cluster, indicating that—globally—the initial calculated conformation remained stable throughout the entire trajectory. It consists of a right-handed α-helix ranging from L-Ala^5 to L-Leu^{10} as judged both visually (Figure 3) and by the position of the phi/psi backbone dihedral angle pairs on a Ramachandran map (Figure S10). This part of the molecule is located between the two anchoring points of the diyne linker. The helical segment is preceded by a single type II β-turn, as judged by the presence of a characteristic hydrogen bond between L-Ala^5 N–H and L-Thr^2 C′. Therefore, it seems that the diyne linker imposes a side chain orientation for L-Ser^4 that prevents its backbone from adopting a helical conformation. As a result, the α-helix is limited to the endocyclic portion of the molecule. Indeed, when visually inspecting the diyne linkage at the N-terminal side, it is clear that the diyne linker should be directed towards the C-terminal (to L-Ser^{11}). However, in reality, the L-Ser^4 has its C$^\alpha$–C$^\beta$ bond pointed towards the N-terminal, as enforced by the stereochemistry of this amino acid. On the basis of this, we expected that **8** (possessing a D-Ser^4) would be able to feature an α-helix extending in the endocyclic portion of the molecule.

For **8**, 166 unambiguous interproton distances, with 27 medium and 26 long-range constants (Table S8), were used to generate a conformation ensemble in solution in exactly the same fashion as for **7**. Here also, all residues were involved in sufficient number of restraints from which a well-defined, converged ensemble of structures could be obtained. Again, a single dominant cluster was found present throughout the refinement MD. As expected, this single conformation features a left-handed α-helix between L-Leu^1 and L-Ser^{11} as judged both visually (Figure 4) and by the position of the phi/psi backbone dihedral angle pairs on a Ramachandran map (Figure S10). Although the overall backbone RMSD between the structures of **7** and **8** is 2.11 Å, that of their common helical peptide segments is only 0.56 Å indicating that the endocylic portions of both molecules are quite similar. The C$^\alpha$–C$^\beta$ bond of D-Ser^4 is directed towards the C-terminus, which is a more suitable orientation to staple the molecule with the diyne linker. This allows the exocyclic amino acid sequence to adopt a helical conformation as well. The higher helical content of **8** vs **7** was confirmed by CD (Figure S12), which supports the NMR data.

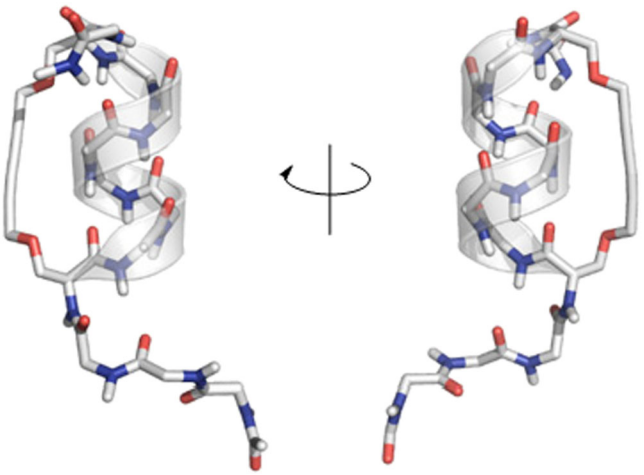

FIGURE 3 Nuclear magnetic resonance (NMR) structure of **7**

Colour online, B&W in print

Colour online, B&W in print

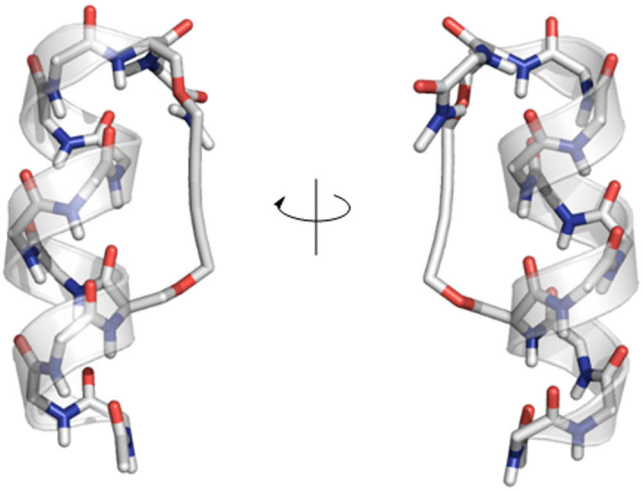

FIGURE 4 Nuclear magnetic resonance (NMR) structure of **8**

4 | CONCLUSIONS

In conclusion, it was found that α-helix stabilization by means of 1,3-diyne stapling is efficient when a combination of side chain propargylated D- and L-Ser residues is deployed in positions *i* and *i* +7, respectively. Whereas macrolactamization by classical carboxylic acid activation seemingly gave the targeted stapled peptides, NMR analysis suggested that epimerization occurred at the level of residue 4, and hence, care must be taken when such macrocyclizations are used to access constrained analogues. Therefore, a conformational analysis by CD only is risky, and additional confirmation by NMR is adequate. In the current study, a thorough structure analysis via NMR and molecular modeling proved that the [L-Ser^{4},L-Ser^{11}] combination only provided a helical structure within the macrocycle, while the exocyclic segment was not part of the helix. In contrast, the [D-Ser^{4},L-Ser^{11}] analogue gratifyingly provided a full α-helix over the entire peptide sequence. Similarly to analogous studies reporting on staples designed to lock helical peptides and wherein differences are noted when different amino acid configurations are applied, this study emphasizes the importance of side chain orientations at the tethering positions.

ACKNOWLEDGEMENTS

The Research Foundation Flanders (FWO Vlaanderen) and the Research Council of the Vrije Universiteit Brussel are acknowledged for the financial support. K.V.H. thanks the Research Foundation Flanders (FWO) for granting a PhD fellowship. K.V.H. and N.G. thank the Hercules Foundation (project AUGE/11/029 "3D-SPACE: 3D Structural Platform Aiming for Chemical Excellence") and the Special Research Fund (BOF)—UGent (project 01N03217) for funding. Benjámin Kovács (NMR and Structure Analysis, UGent) is thanked for useful discussions regarding MD simulations and subsequent cluster analysis. The 700 MHz equipment used in this work is part of the NMR Expertise Centre at UGent and funded by the BOF fund of UGent and the FFEU-ZWAP initiative of the Flemish Government.

ORCID

Steven Ballet https://orcid.org/0000-0003-4123-1641

REFERENCES

1. Pelay-Gimeno M, Glas A, Koch O, Grossmann TN. Structure-based design of inhibitors of protein–protein interactions: mimicking peptide binding epitopes. *Angew Chem Int Ed*. 2015;54(31):8896-8927. https://doi.org/10.1002/anie.201412070
2. Nevola L, Giralt E. Ppi Chem Comm. *Chem Commun*. 2015;51(16):3302-3315. https://doi.org/10.1039/C4CC08565E
3. Bullock BN, Jochim AL, Arora PS. Assessing helical protein interfaces for inhibitor design. *J Am Chem Soc*. 2011;133(36):14220-14223. https://doi.org/10.1021/ja206074j
4. Arkin MR, Wells JA. Small-molecule inhibitors of protein-protein interactions: progressing towards the dream. *Nat Rev Drug Discov*. 2004;3(4):301-317. https://doi.org/10.1038/nrd1343
5. Wilson AJ. Inhibition of protein–protein interactions using designed molecules. *Chem Soc Rev*. 2008;38(12):3289-3300. https://doi.org/10.1039/b807197g
6. Gross A, Hashimoto C, Sticht H, Eichler J. Synthetic peptides as protein mimics. *Front Bioeng Biotechnol*. 2016;3:1-16. https://doi.org/10.3389/fbioe.2015.00211
7. White CJ, Yudin AK. Contemporary strategies for peptide macrocyclization. *Nat Chem*. 2011;3(7):509-524. https://doi.org/10.1038/nchem.1062
8. Dougherty PG, Qian Z, Pei D. Macrocycles as protein-protein interaction inhibitors. *Biochem J*. 2017;474(7):1109-1125. https://doi.org/10.1042/BCJ20160619
9. Kutchukian PS, Yang JS, Verdine GL, Shaknovich EI. All-atom model for stabilization of α-helical structure in peptides by hydrocarbon staples. *J Am Chem Soc*. 2009;131(13):4622-4627. https://doi.org/10.1021/ja805037p
10. Lau YH, de Andrade P, Wu Y, Spring DR. Peptide stapling techniques based on different macrocyclisation techniques. *Chem Soc Rev*. 2015;44(1):91-102. https://doi.org/10.1039/C4CS00246F
11. Schafmeister CE, Po J, Verdine GL. An all-hydrocarbon cross-linking system for enhancing the helicity and metabolic stability of peptides. *J Am Chem Soc*. 2000;122(24):5891-5892. https://doi.org/10.1021/ja000563a
12. Fujimoto K, Oimoto N, Katsuno K, Inouye M. Effective stabilisation of α-helical structures in short peptides with acetylenic cross-linking agents. *Chem Commun*. 2004;0(11):1280-1281. https://doi.org/10.1039/B403615H
13. Jackson DY, King DS, Chmielewski J, Singh S, Schultz PG. General approach to the synthesis of short alpha-helical peptides. *J Am Chem Soc*. 1991;113(24):9391-9392. https://doi.org/10.1021/ja00024a067
14. Woolley GA. Photocontrolling peptide α helices. *Acc Chem Res*. 2005;38(6):486-493. https://doi.org/10.1021/ar040091v
15. Renner C, Moroder L. Azobenzene as conformational switch in model peptides. *Chembiochem*. 2006;7(6):868-878. https://doi.org/10.1002/cbic.200500531
16. Phelan JC, Skelton NJ, Braisted AC, McDowell RS. A general method for constraining short peptides to an α-helical conformation. *J Am Chem Soc*. 1997;119(3):455-460. https://doi.org/10.1021/ja9611654
17. Sia SK, Carr PA, Cochran AG, Malshkevich VN, Kim PS. Short constrained peptides that inhibit HIV-1 entry. *Proc Natl Acad Sci U S A*. 2002;99(23):14664-14669. https://doi.org/10.1073/pnas.232566599

18. Lau YH, de Andrade P, McKenzie GJ, Venkitaraman AR, Spring DR. Linear aliphatic dialkynes as alternative linkers for double-click stapling of P53-derived peptides. *Chembiochem*. 2014;15(18):2680-2683. https://doi.org/10.1002/cbic.201402374
19. Lau YH, de Andrade P, Quah S-T, et al. Functionalised staple linkages for modulating the cellular activity of stapled peptides. *Chem Sci*. 2014;5(5):1804-1809. https://doi.org/10.1039/C4SC00045E
20. Muppidi A, Wang Z, Li X, Chen J, Lin Q. Achieving cell penetration with distance-matching cysteine cross-linkers: a facile route to cell-permeable peptide dual inhibitors of Mdm2/Mdmx. *Chem Commun*. 2011;47(33):9396-9398. https://doi.org/10.1039/C1CC13320A
21. Muppidi A, Doi K, Edwardraja S, et al. Rational design of proteolytically stable, cell-permeable peptide-based selective Mcl-1 inhibitors. *J Am Chem Soc*. 2012;134(36):14734-14737. https://doi.org/10.1021/ja306864v
22. Fujimoto K, Kajino M, Inouye M. Development of a series of cross-linking agents that effectively stabilize α-helical structures in various short peptides. *Chem Eur J*. 2008;14(3):857-863. https://doi.org/10.1002/chem.200700843
23. Blackwell HE, Grubbs RH. Highly efficient synthesis of covalently cross-linked peptide helices by ring-closing metathesis. *Angew Chem Int Ed*. 1998;37(23):3281-3284. https://doi.org/10.1002/(SICI)1521-3773(19981217)37:23<3281::AID-ANIE3281>3.0.CO;2-V
24. Kim Y-W, Kutchukian PS, Verdine GL. Introduction of all-hydrocarbon *i*,*i*+3 staples into α-helices via ring-closing olefin metathesis. *Org Lett*. 2010;12(13):3046-3049. https://doi.org/10.1021/ol1010449
25. Verlinden S, Geudens N, Martins JC, Tourwé D, Ballet S, Verniest G. Oxidative α,ω-diyne coupling as an approach towards novel peptidic macrocycles. *Org Biomol Chem*. 2015;13(36):9398-9404. https://doi.org/10.1039/C5OB01153A
26. Verlinden S, Ballet S, Verniest G. Synthesis of heterocycle-bridged peptidic macrocycles through 1,3-diyne transformations. *Eur J Org Chem*. 2016;2016(35):5807-5812. https://doi.org/10.1002/ejoc.201601215
27. Maza JC, Howard CA, Vipani MA, Travis CR, Young DD. Utilization of alkyne bioconjugations to modulate protein function. *Bioorg Med Chem Lett*. 2017;27(1):30-33. https://doi.org/10.1016/j.bmcl.2016.11.041
28. Silvestri AP, Cistrone PA, Dawson PE. Adapting the Glaser reaction for bioconjugation: robust access to structurally simple, rigid linkers. *Angew Chem Int Ed*. 2017;56(35):10438-10442. https://doi.org/10.1002/anie.201705065
29. Cistrone PA, Silvestri AP, Hintzen JCJ, Dawson PE. Rigid peptide macrocycles from on-resin Glaser stapling. *Chembiochem*. 2018;19(10):1031-1035. https://doi.org/10.1002/cbic.201800121
30. Pribylka A, Krchnak V. An alkyne rod to constrain a peptide backbone in an extended conformation. *Eur J Org Chem*. 2018;2018(34):4709-4715. https://doi.org/10.1002/ejoc.201800979
31. Hu B, Gilkes DM, Chen J. Efficient P53 activation and apoptosis by simultaneous disruption of binding to MDM2 and MDMX. *Cancer Res*. 2007;67(18):8810-8817. https://doi.org/10.1158/0008-5472.CAN-07-1140
32. Chang YS, Graves B, Guerlavais V, et al. Stapled α-helical peptide drug development: a potent dual inhibitor of MDM2 and MDMX for P53-dependent cancer therapy. *Proc Natl Acad Sci U S A*. 2013;110(36):3445-3454. https://doi.org/10.1073/pnas.1303002110
33. Nguyen BD, Meng X, Donovan KJ, Shaka AJ. SOGGY. *J Magn Reson*. 2007;184(2):263-274. https://doi.org/10.1016/j.jmr.2006.10.014
34. Humphrey W, Dalke A, Schulten K. VMD—visual molecular dynamics. *J Molec Graphics J Mol Graph*. 1996;14(1):33-38. https://doi.org/10.1016/0263-7855(96)00018-5
35. Roe DR, Cheatham TE. PTRAJ and CPPTRAJ: Software for Processing and Analysis of Molecular Dynamics Trajectory Data. *J Chem Theory Comput*. 2013;9(7):3084-3095. https://doi.org/10.1021/ct400341p
36. Cantel S, Desgranges S, Martines J, Fehrentz J-A. Saponification of esters of chiral α-amino acids anchored through their amine function on solid support. *J Pept Sci*. 2004;10(6):326-328. https://doi.org/10.1002/psc.561
37. Vrancken WF, Boucher W, Stevens TJ, et al. CCPN. *Proteins*. 2005;59(4):687-696. https://doi.org/10.1002/prot.20449
38. Geudens N, Nasir MN, Crowet J-M, et al. Membrane Interactions of Natural Cyclic Lipodepsipeptides of the Viscosin Group. *Biochim Biophys Acta Biomembr*. 1859;2017(3):331-339. https://doi.org/10.1016/j.bbamem.2016.12.013

SUPPORTING INFORMATION

Additional supporting information may be found online in the Supporting Information section at the end of the article.

How to cite this article: Verlinden S, Geudens N, Van holsbeeck K, et al. The 1,3-diyne linker as a rigid "*i*,*i*+7" staple for α-helix stabilization: Stereochemistry at work. *J Pep Sci*. 2019;e3194. https://doi.org/10.1002/psc.3194